IC/99/13

# Distinguishing the Higgs scalars of NMSSM and Z′ models for large Higgs trilinear couplings

D. A. Demir
*The Abdus Salam International Centre for Theoretical Physics, I-34100 Trieste, Italy*
(February 1, 2008)



## Abstract

Two well-known extended supersymmetric models, $Z'$ models and NMSSM, are comparatively analyzed in the limit of large trilinear Higgs couplings. The two models are found to have distinguishable Higgs spectra at both tree- and loop- levels. Higgs production through Bjorken processes at an $e^+e^-$ collider is shown to discriminate between the two models.

## I. INTRODUCTION

A proper understanding of the basic mechanism of the electroweak symmetry breaking is one of the central problems in particle physics. If the fundamental particles are to remain weakly interacting up to high energies the symmetry breaking sector of the model should contain one or more scalar Higgs bosons with masses of the order of weak scale $\sim G_F^{-1/2}$. The simplest mechanism for the breaking of the electroweak symmetry is realized in the SM where one scalar field remains in the spectrum, manifesting itself as the physical Higgs particle $H$. Though the scalar sector of the SM is simple enough to predict just one Higgs boson, it has been criticized from various theoretical aspects, the most common of which is the quadratic divergence of the Higgs mass. This naturalness problem has triggered the study of supersymmetric models. MSSM, being the simplest of such models, lacks an explanation for the origin and scale of the bilinear Higgs coupling mass, which is commonly known as the $\mu$ problem. In connection with this last point, extended supersymmetric models, in which bilinear Higgs coupling mass $\mu$ is related to the vacuum expectation value of some SM gauge singlet, have been proposed. In these extended models, one extends either merely the Higgs sector (NMSSM) [1] , or both Higgs sector and the SM gauge group ($Z'$ models) [2–4], and these generally lead to a larger Higgs spectrum.Thus, in accelerator searches of the Higgs, even if detected, it will still be a challenging issue to determine what kind of model it implies. Consequently, it is desirable to investigate the possibility of discriminating between these models given that some spectrum of Higgs particles are observed at some ($e^+e^-$) collider.

High precision electroweak data indicate a preference for Higgs boson to have a mass within a factor of 2 or so of 140 GeV [5]. However, weak (logarithmic) dependence of the theoretical predictions on the Higgs boson mass as well as the intrinsic uncertainities in the electroweak observables prevent to derive stringent predictions for the Higgs mass, and literally almost the entire SM Higgs boson range (up to and above $\sim 1$ TeV) must be swept for the Higgs search [6]. From the direct searches, four LEP experiments put the lower bound of 95 GeV for the Higgs mass [7]. The dominant production mechanism for Higgs boson within the LEP2 reach is the Higgs strahlung process, $e^+e^- \to ZH$, in which Higgs boson is emitted from a virtual $Z$ line. This process has already been analyzed in SM [8] and MSSM [9], including the radiative corrections. One notes that for $\nu_e\bar{\nu}_e$ and $e^+e^-$ in the final state, fusion process where Higgs boson is formed in $WW$ and $ZZ$ t-channel collisions will interfere with the Higgs- strahlung amplitude.

In this work we analyze NMSSM and $Z'$ models comparatively with particular emphasis on their CP–even Higgs spectra. To have direct effects of these particles at the weak scale one demands the gauge singlet scalar to have a vacuum expectation value (VEV) around the weak scale. Such a breaking scheme leading relatively light particles (including the $Z'$ boson itself) has already been shown to exist in $Z'$ models [2]. This occurs when the trilinear coupling of the Higgs doublets and the singlet in the soft supersymmetry breaking terms becomes large compared to the soft masses, and leads to appoximately equal VEV's for both doublets and the singlet. This type of vacuum state satisfies the existing constraints on the mixing between the $Z^0$ and $Z'$, and produces a spectrum of scalars at the weak scale.

However, in NMSSM such Higgs trilinear coupling driven minima, though can exist, are not required by some phenomenological requirement [1] as in the $Z'$ models [2]. In $Z'$ models for singlet to have large VEV one needs the singlet mass-squared to be large negative. In

NMSSM, in addition to this mechanism, one can allow for the singlet trilinear coupling to be large negative to have a large singlet VEV. The opposite limit, namely, the requirement of having both singlet and the doublet VEV's to be around the weak scale could be satisfied by choosing the mass-squareds of the Higgs fields appropriately, in particular, letting them be sufficiently larger than both singlet cubic coupling and Higgs trilinear coupling, in absolute magnitude. However,this requirement can also be met by choosing Higgs trilinear coupling large enough compared to soft masses and singlet cubic coupling.

In this work we will perform a comparative study of NMSSM and $Z'$ models in the same kind of minimum induced by the relatively large values of the Higgs trilinear coupling. In particular, we dicuss the CP–even spectra, and investigate their collider signature, both at tree– and loop– levels, by analyzing the Higgs production through the Bjorken processes.

In Sec.2 we derive the couplings and masses of the scalars, and specify all of the relevant properties of NMSSM and $Z'$ models. We also discuss vacuum stability and scalar spectrum against radiative corrections.

In Sec.3 we give a comparative discussion of the electron-positron annihilation to four-fermion final states through Higgs-strahlung in both NMSSM and $Z'$ models with reference to the corresponding SM expressions.

In Sec. 4 we conclude the work.

## II. SCALAR SECTORS OF NMSSM AND $Z'$ MODELS

We consider a supersymmetric model whose scalar sector consists of two Higgs doublets $\hat{H}_1$, $\hat{H}_2$, and a SM-singlet $\hat{S}$. NMSSM is such a supersymmetric model whose scalar sector is spanned by these fields, and gauge symmetry is exactly that of the MSSM. In fact, it is specified by the superpotential

$$W \ni h_s \hat{S}\, \hat{H}_1 \cdot \hat{H}_2 + \frac{1}{3} k_s \hat{S}^3 + h_t \hat{U}^c \hat{Q} \cdot \hat{H}_2 \tag{1}$$

where contributions of all fermions but the top quark are neglected as they are much lighter. Here $\hat{Q}$ and $\hat{U}^c$ are left-handed SU(2) doublet and singlet quark superfields. The cubic term in (1) is necessary to avoid the unwanted Peccei-Quinn symmetry. However, superpotential has still a $Z_3$ symmetry which, when spontaneously broken, causes serious problems about domain walls [10]. This problem can be avoided by the addition of non-renormalizable terms of the form $(\hat{S}/M_P)^n \hat{S}\hat{H}_1 \cdot \hat{H}_2$ if gravity violates the $Z_3$ symmetry [11]. Despite these problems, the superpotential (1) is sufficient to understand the basic implications of NMSSM for particle physics applications.

Besides NMSSM, $Z'$ models, which are those models having a low-energy supersymmetric extra U(1) factor, have also an extended scalar sector compared to MSSM. Unlike NMSSM, these models are devoid of such cosmological problems, and are predicted in string compactifications and $E(6)$ GUT's [2,4,12]. In $Z'$ models, not only the scalar sector but also the gauge sector is extended by an extra $U(1)$ factor with the coupling $g_{Y'}$. Consequently, all fields are charged under this group, and we make the charge assignment $Q_1$, $Q_2$, $Q_S$, $Q_Q$ and $Q_U$ for $\hat{H}_1$, $\hat{H}_2$, $\hat{S}$, $\hat{Q}$, and $\hat{U}^c$, respectively. In this case, the superpotential is given by

$$W \ni h_s \hat{S}\, \hat{H}_1 \cdot \hat{H}_2 + h_t \hat{U}^c \hat{Q} \cdot \hat{H}_2 \tag{2}$$

where a cubic term is forbidden due to the extra Abelian group factor. Formally, one can obtain this superpotential by setting $k_s = 0$ in (1). Although the superpotentials (1) and (2) formally differ only by the cubic term, resulting scalar potentials reveal explicitly the difference between the two models, through F- and D- terms. In fact, the most general representation for the scalar potential is given by

$$\begin{aligned} V = & m_1{}^2 \mid H_1 \mid^2 + m_2{}^2 \mid H_2 \mid^2 + m_S{}^2 \mid S \mid^2 + \lambda_1 \mid H_1 \mid^4 + \lambda_2 \mid H_2 \mid^4 \\ & + \lambda_S \mid S \mid^4 + \lambda_{12} \mid H_1 \mid^2 \mid H_2 \mid^2 + \lambda_{1S} \mid H_1 \mid^2 \mid S \mid^2 + \lambda_{2S} \mid H_2 \mid^2 \mid S \mid^2 \\ & + \tilde{\lambda}_{12} \mid H_1^\dagger H_2 \mid^2 + \lambda_{S12}(S^2 H_1.H_2 + H.c.) - h_s A_s (S H_1.H_2 + H.c.) \\ & - k_s A_k (S^3 + H.c.) \end{aligned} \tag{3}$$

where the dimensionless $\lambda$ coefficients are listed in Table I for both models. In writing this potential we suppressed the contribution of the squarks for simplicity, however, when discussing the loop effects we will explicitly take them into account.

For later use we parametrise the vacuum expectation values of the Higgs fields as follows:

$$< H_1 >= \frac{1}{\sqrt{2}} \begin{pmatrix} v_1 \\ 0 \end{pmatrix} \ , \ < H_2 >= \frac{1}{\sqrt{2}} \begin{pmatrix} 0 \\ v_2 \end{pmatrix} \ , \ < S >= \frac{v_s}{\sqrt{2}} \tag{4}$$

with real $v_1, v_2$ and $v_s$. All physical quantities of interest can be expressed in terms of parameters of the potential and these VEV's.

### A. Couplings of Vector Bosons to Fermions

Before specializing to a particular minimum of the potential we derive vector boson-fermion couplings as they are essentially independent of the scalar sector of the model. Since the vector boson sector of the $Z'$ model is larger we analyze it in detail first, and then infer the necessary formulae for NMSSM. There are two massive neutral vector bosons in $Z'$ models, the usual $Z$ of the SM gauge group, and $Z'$ of the extra $U(1)$ group, which mix through the mass-squared matrix:

$$(\mathcal{M}^2)_{Z-Z'} = \begin{pmatrix} M_Z^2 & \Delta^2 \\ \Delta^2 & M_{Z'}^2 \end{pmatrix}, \tag{5}$$

whose entries are given by

$$M_Z^2 = \frac{1}{4} G^2 (v_1^2 + v_2^2), \tag{6}$$

$$M_{Z'}^2 = g_{Y'}^2 (v_1^2 Q_1^2 + v_2^2 Q_2^2 + v_s^2 Q_S^2), \tag{7}$$

$$\Delta^2 = \frac{1}{2} g_{Y'}\, G (v_1^2 Q_1 - v_2^2 Q_2), \tag{8}$$

where $G^2 = g_2^2 + g_Y^2$. $Z - Z'$ mixing angle, which is one of the most important parameters in $Z'$ models, is defined by

$$\tan 2\theta = -\frac{2\Delta^2}{M_{Z'}^2 - M_Z^2} \tag{9}$$

Diagonalization of $(\mathcal{M}^2)_{Z-Z'}$ leads to mass-eigenstates $Z_1$ and $Z_2$ with masses $M_{Z_1}$ and $M_{Z_2}$, respectively. The $Z-Z'$ mixing angle forms the mere sign of $Z'$ models in LEP Z-pole data and, in fact, in this way it is constrained to be $\lesssim 10^{-3}$ [2]. Actually the way $\theta$ enters the LEP Z-pole observables can be seen through the $Z_1 f\bar{f}$ couplings. For a fermion $f$, we define

$$\epsilon^f = I_3^f - Q_{em}^f \sin^2\theta_W \ , \ \epsilon'^f = Q_f \tag{10}$$

where $I_3^f$ is the third component of the weak isospin, and $Q_{em}^f$ is the electric charge. Then coupling of $Z_i$ to a fermion line is given by the lagrangean

$$\mathcal{L}_i = \frac{G}{2} Z_i^\mu \bar{f}\gamma_\mu (g_V^{(i)} - \gamma_5 g_A^{(i)}) f \tag{11}$$

where vector coupling $g_V^{(i)}$ and axial coupling $g_A^{(i)}$ are listed in Table II for $Z'$ models. One notices that $g_V^{(i)}$ depends on the sum of the extra U(1) charges of the left–handed fermion doublet and right–handed SU(2) singlet, that is, $Q_{f_L} + Q_{f_R}$. Due to the gauge invariance of the superpotential this sum equals minus the extra U(1) charge of the associated Higgs doublet. Hence it is not possible to implement the leptophobic $Z'$ models though it is required by the high energy precision data. Nevertheless, this problem can be sidestepped if lepton charges under extra U(1) group vanish, and there is no trilinear mass term in the superpotential for leptons, that is, they acquire masses through the non-renormalizable interactions as all light quarks are supposed to do [16]. Thus we rectrict our attention particularly to the top Yukawa coupling given in the superpotential (2). Unlike the vector couplings, axial couplings depend on the difference between the extra U(1) charges of the doublet and SU(2)-singlet fermions. Needless to say, in the limit of small mixing angles, $Z_1 f\bar{f}$ couplings approach the corresponding SM ones. In NMSSM, one has only the standard $Z$ boson whose couplings can be obtained by setting $g_{V,A}^{(2)} = 0$, $g_{Y'} = 0$, and $\theta = 0$ in Table II. NMSSM couplings can be compared with the results of [1].

### B. Couplings of Vector Bosons to CP-even Higgs Bosons

After obtaining the couplings of vector bosons to fermions, now we turn to the discussion of CP-even Higgs-vector boson couplings which are of fundamental importance in discussing the Higgs production through the Higgs-strahlung type processes. Evaluation of the couplings of Higgs bosons to vector bosons requires the minimization of the potential (3) after which one obtains the physical particle spectrum together with the necessary diagonalizing matrices. Each of the models under concern has its own phenomenological constraints to be satisfied. As discussed in the Introduction, in the case of NMSSM, one should prevent the creation of a pseudoscalar Goldstone mode, which can easily be satisfied for non-vanishing $k_s A_k$. In the case of $Z'$ models, however, one has stringent constraints on the possible vacuum state, that is, the $Z-Z'$ mixing angle (9) should be $\lesssim 10^{-3}$ [2], and $Z'$ mass must be $\gtrsim$ 600 GeV, as required by the recent Tevatron direct search with leptonic final states [13]. As long as one considers the case of leptophobic $Z'$ in accord with the LEP Z-pole data, this latter condition can be relaxed. However, the former one is a non-trivial condition on the possible vacua of $Z'$ models. In the next section we shall analyze the relevant vacuum state of the two models in detail.

For the models under concern, to have spectacular effects at LEP2 and NLC energies, the breaking scale of the supersymmetry is expected to be around the weak scale. Indeed, when the supersymmetry is broken above $\sim$ TeV, at the weak scale one ends up with an effective 2HDM [14,15] which carries only indirect information about the underlying model. Thus, in what follows we assume supersymmetry to be broken around the weak scale for both models under concern. This observation requires all three VEV's to be around the weak scale. In particular, $-m_S^2 >> |m_{1,2}^2|$ is prohibited in both models as otherwise SM-singlet $S$ may acquire a large VEV. In NMSSM, in addition to this, one has to prevent $|k_s A_k| >> |h_s A_s|$ as the former one can induce a large VEV for $S$ through the cubic soft term.

*1. Relevant minimum in $Z'$ models*

We first discuss $Z'$ models, and following it we turn to the discussion of NMSSM. In analyzing the $Z'$ models the basic quantity of interest is the $Z - Z'$ mixing angle (9) which has to be small to satisfy the present phenomenological bounds [2]. An observation on (9) reveals that $Z - Z'$ mixing angle $\theta$ can be made small either by choosing $M_{Z'} >> M_Z$, or by forcing $\Delta^2$ itself to be small without constraining $M_{Z'}$. While the former one requires SM-singlet VEV to be much larger than the doublet VEV's, the latter allows all three VEV's to be of the same order of magnitude, as required by the discussions at the end of the last subsection. One can realize small $\Delta^2$ when the charges of the Higgs doublets under extra U(1) are equal, and Higgs trilinear coupling $h_s A_s$ is larger than the other mass parameters [2,4]. We name that minimum of the potential (3) for which $h_s A_s$ is larger than the other mass parameters as Higgs trilinear coupling driven minimum (HTCDM) from now on. In fact, the potential possesses a HTCDM when $A_s$ exceeds the critical point

$$A_s^{crit} = \sqrt{\frac{8}{3} m^2} \tag{12}$$

where $m^2 = m_1^2 + m_2^2 + m_S^2$. As this formula indicates, when $m^2 > 0$, $A_s^{crit}$ exists, and passage of the potential from small to large trilinear coupling regime is a first order phase transition, namely, all VEV's are discontinuous at $A_s^{crit}$. On the other hand, when $m^2 < 0$, there is no critical point at all; transition is exclusively second order [2,4]. However, independent of the sign of $m^2$ and the order of the transition, in the limit of large $A_s$, all VEV's converge the solution

$$v_1 \sim v_2 \sim v_s \sim \frac{A_s}{\sqrt{2} h_s} \tag{13}$$

with which one can fix $A_s = h_s (2G_F)^{-1/2}$ by using the $W^{\pm}$ mass. When the potential (3) possesses a HTCDM, in the basis $(Re[H_1^0], Re[H_2^0], Re[S^0])^T$, CP-even Higgs mass-squared matrix is given by

$$(\mathcal{M}^2)_h = (G_F^{-1}/4) \begin{pmatrix} 2\lambda_1 + h_s^2 & \lambda_{12} - h_s^2 & \lambda_{1S} - h_s^2 \\ \lambda_{12} - h_s^2 & 2\lambda_2 + h_s^2 & \lambda_{2S} - h_s^2 \\ \lambda_{1S} - h_s^2 & \lambda_{2S} - h_s^2 & 2\lambda_S + h_s^2 \end{pmatrix} \tag{14}$$

where $\lambda_1 = \lambda_2$ and $\lambda_{1S} = \lambda_{2S}$, because $Q_1 = Q_2$ as assumed above, when discussing HTCDM. Diagonalization of the CP-even Higgs mass-squared matrix gives the following mass spectrum

$$m_{h_1} = (G_F^{-1/2}/2)h_s \ , \ m_{h_2} = (G_F^{-1/2}/2)\sqrt{h_s^2 + G^2/2} \ , \ m_{h_3} = (G_F^{-1/2}/2)\sqrt{6g_{Y'}^2 + h_s^2} \qquad (15)$$

in the increasing order. The physical mass eigenstates $(h_1, h_2, h_3)^T$ are related to the basis vector $(Re[H_1^0], Re[H_2^0], Re[S^0])^T$ via the diagonalizing matrix

$$\mathcal{R} = \begin{pmatrix} 1/\sqrt{3} & 1/\sqrt{3} & 1/\sqrt{3} \\ -1/\sqrt{2} & 1/\sqrt{2} & 0 \\ -1/\sqrt{6} & -1/\sqrt{6} & 2/\sqrt{6} \end{pmatrix} \qquad (16)$$

Having matrix $\mathcal{R}$ at hand, one can easily compute the coupling strengths of $h_k$ to $Z_i Z_j$ for $i, j = 1, 2$ and $k = 1, 2, 3$. In fact, Table III gives a list of these couplings for all possible cases. As one notices this table has important implications for the mechanism of Higgs production through the Higgs-strahlung type processes. First of all, the sum of the squared $h_k Z_1 Z_1$ couplings equals the square of the SM $H\,Z\,Z$ coupling. Thus, just like MSSM, mixings in the scalar sector result in a reduction of the coupling strength, implying a smaller production cross section than that of the SM.

Next, one observes that some couplings vanish. While $h_1$ and $h_3$ have only diagonal couplings in the form $Z_i Z_i$, $h_2$ has only $Z_1 Z_2$ type coupling. Hence, in a transition of the form $Z_i \to h_k Z_j$, if the initial and final vector bosons are identical then only lightest and heaviest Higgs bosons could be radiated off. Unlike this, if vector bosons are not identical, then the radiated scalar can only be next-to-lightest Higgs. This well defined spectrum of the produced scalars may be important in a particular collider search, say LEP2 or NLC. This completes the discussion of the scalar sector of the $Z'$ models at the tree level. When we discuss the loop effects we shall reanalyze some quantities derived in this section.

### C. Relevant minimum in NMSSM

Having discussed the scalar sector of the $Z'$ models, we now start analyzing NMSSM scalar potential (3) in reference to Table I. As mentioned at the beginning of this section, we require supersymmetry be broken around the weak scale, and thus, Higgs VEV's are of the same order of magnitude. Restrictions on $Z'$ models do not have any analogue in NMSSM, and one is generally free to realize any kind of minimum as long as VEV's do not have too big splittings among them. In fact, all relevant portions of the NMSSM parameter space have already been analyzed in [1] whose results will not be reproduced here. For a comparative and parallel study of the $Z'$ models and NMSSM, it would be convenient to discuss the latter one in that portion of the parameter space required by the former as it is severely constrained by the LEP Z-pole data. Thus, differently than [1], we shall discuss NMSSM also in the limit of large Higgs trilinear coupling. Actually, NMSSM scalar potential (3) would possess a HTCDM provided that $|h_s A_s + k_s A_k|$ exceeds the critical value

$$\tilde{A}_s^{crit} = \sqrt{\frac{8}{9}\lambda m^2} \qquad (17)$$

where $\lambda = 3h_s^2 + k_s^2 + 2h_s k_s$, and $m^2 = m_1^2 + m_2^2 + m_S^2$. In NMSSM, instead of $|h_s A_s|$, one has $|h_s A_s + k_s A_k|$ characterizing the minimum of the potential. At this point one should bare in mind that $S^3$ coupling $|k_s A_k|$ singles out $S$ and its large values automatically creates $v_s >> v_{1,2}$, rather than $v_1 \sim v_2 \sim v_s$. Consequently, if one wishes to obtain a HTCDM for the potential (3), $|k_s A_k|$ must be much less than $|h_s A_s|$ so that $\tilde{A}_s^{crit}$ approximately applies to $A_s^{crit}$. This is an approximate statement because one cannot ignore $|k_s A_k|$ completely due to the axion problem mentioned in the Introduction. Just like the $Z'$ models, type of the transition is sensitive to the sign of $m^2$, however, independent of this, for large enough $|h_s A_s|$, all VEV's converge to the same value given by

$$v_1 \sim v_2 \sim v_s \sim \frac{3}{\lambda}\frac{h_s A_s + k_s A_k}{\sqrt{2}} \tag{18}$$

which mainly follows $h_s A_s$ since $|k_s A_k| << |h_s A_s|$. An analysis of the $Z'$ models reveals that CP-even Higgs mass-squared matrix is highly sensitive to gauge and Yukawa couplings as can be seen from (14). In NMSSM, the prescription $|k_s A_k| << |h_s A_s|$ implies two distinct cases to be analyzed in detail:

$$|k_s A_k| << |h_s A_s| \Longrightarrow \begin{cases} k_s \approx h_s \ \ and \ \ |A_k| << |A_s| \Longrightarrow \text{NMSSM1} \\ k_s << h_s \ \ and \ \ |A_k| \approx |A_s| \Longrightarrow \text{NMSSM2} \end{cases} \tag{19}$$

where we named the two cases as NMSSM1 and NMSSM2 for later use. It is convenient to discuss the implications of these two cases seperately.

NMSSM1 :

In this case one can replace $k_s$ by $h_s$ so that $\lambda \approx 6h_s^2$. Furthermore, neglecting $A_k$ in comparison with $A_s$, one obtains

$$A_s^{crit} \approx \sqrt{2} \times \sqrt{\frac{8}{3}m^2} \tag{20}$$

which, when sufficiently exceeded by $A_s$, implies the VEV's

$$v_1 \sim v_2 \sim v_s \sim \frac{1}{2} \times \frac{A_s}{h_s\sqrt{2}} \tag{21}$$

With these VEV's, in the basis $(Re[H_1^0], Re[H_2^0], Re[S^0])^T$, mass-squared matrix for CP-even scalars turns out to be

$$(\mathcal{M}^2)_h = (G_F^{-1}/4)\begin{pmatrix} G^2/4 + 3h_s^2/2 & -G^2/4 + h_s^2/2 & 0 \\ -G^2/4 + h_s^2/2 & G^2/4 + 3h_s^2/2 & 0 \\ 0 & 0 & 4h_s^2 \end{pmatrix} \tag{22}$$

the diagonalization of which yields Higgs spectrum with masses

$$m_{h_1} = (G_F^{-1/2}/2\sqrt{2})\sqrt{h_s^2 + G^2} \ \ , \ m_{h_2} = (G_F^{-1/2}/\sqrt{2})h_s \ \ , \ m_{h_3} = (G_F^{-1/2})h_s \tag{23}$$

in the increasing order. The physical mass eigenstates $(h_1, h_2, h_3)^T$ are related to the basis vector $(Re[H_1^0], Re[H_2^0], Re[S^0])^T$ via the diagonalizing matrix

$$\mathcal{R} = \begin{pmatrix} -1/\sqrt{2} & 1/\sqrt{2} & 0 \\ 1/\sqrt{2} & 1/\sqrt{2} & 0 \\ 0 & 0 & 1 \end{pmatrix} \tag{24}$$

As this diagonalizing matrix shows, the heaviest Higgs gets contributions only from $Re[S^0]$, and the lighter Higgs particles get contributions only from the neutral CP-even components of $H_1$ and $H_2$. In this sense doublets and the singlet decouple, and produce their Higgs spectra. One recalls that the situation in $Z'$ models was different; there it was only the next-to-lightest Higgs that was independent of $Re[S^0]$. This forms a clear distinction between the two models. With $\mathcal{R}$ matrix at hand, it is easy to compute the strength of the coupling between a $Z$ line and a CP-even Higgs as already listed in the first column of Table IV. As the table shows only next-to-lightest Higgs is radiated off a $Z$ line, and the lightest and the heaviest Higgs scalars cannot be produced. In this way one concludes that Higgs-strahlung type processes can lead to the production of next-to-lightest Higgs only. Moreover, in terms of $Z_1$ couplings, $Z'$ models and NMSSM are complementary to each other. This completes the discussion of the NMSSM1 in terms of its particle spectrum and implications for Bjorken production of the Higgs particles.

NMSSM2 :

In this case one can replace $A_k$ by $A_s$ and neglect $k_s$ in comparison with $h_s$ so that $\lambda \approx 3h_s^2$. Then, in exact similarity with the $Z'$ models, one gets

$$A_s^{crit} \approx \sqrt{\frac{8}{3}m^2} \tag{25}$$

which, when sufficiently exceeded by $A_s$, implies the VEV's

$$v_1 \sim v_2 \sim v_s \sim \frac{A_s}{h_s\sqrt{2}} \tag{26}$$

With these VEV's, in the basis $(Re[H_1^0], Re[H_2^0], Re[S^0])^T$, mass-squared matrix for CP-even scalars turns out to be

$$(\mathcal{M}^2)_h = (G_F^{-1}/4) \begin{pmatrix} G^2/4 + h_s^2 & -G^2/4 & 0 \\ -G^2/4 & G^2/4 + h_s^2 & 0 \\ 0 & 0 & h_s^2 \end{pmatrix} \tag{27}$$

the diagonalization of which yields the particle spectrum

$$m_{h_1} = (G_F^{-1/2}/2)h_s \ , \ m_{h_2} = (G_F^{-1/2}/2)\sqrt{h_s^2 + 2k_s^2} \ , \ m_{h_3} = (G_F^{-1/2}/2)\sqrt{h_s^2 + G^2/2} \ , \tag{28}$$

in the increasing order. The physical mass eigenstates $(h_1, h_2, h_3)^T$ are related to the basis vector $(Re[H_1^0], Re[H_2^0], Re[S^0])^T$ via the diagonalizing matrix

$$\mathcal{R} = \begin{pmatrix} 1/\sqrt{2} & 1/\sqrt{2} & 0 \\ 0 & 0 & 1 \\ -1/\sqrt{2} & 1/\sqrt{2} & 0 \end{pmatrix} \tag{29}$$

In comparison with NMSSM1, here one encounters some novel aspects. Though the CP-even Higgs mass-squared matrices (27) and (22) have the same form their dependences on $h_s^2$ are not identical because of the fact that $k_s$ plays different roles in two cases. However, one still expects doublets and the singlet to decouple due to the form of the mass-squared matrix (27). Indeed, as the diagonalizing matrix (29) shows this time it is the next-to-lightest Higgs that is a pure singlet state as opposed to NMSSM1 where the heaviest Higgs was a pure singlet. One notices that since $k_s << h_s$, $h_1$ and $h_2$ are nearly degenerate in mass. A comparison of the diagonalizing matrices (24) and (29) implies the cyclic interchange $h_3 \longleftrightarrow h_2$, $h_2 \longleftrightarrow h_1$ , and $h_1 \longleftrightarrow h_3$. Thus, in NMSSM2 $h_2$ is a pure singlet, and the heaviest and the lightest Higgs particles get contribution from only the neutral CP-even parts of the Higgs doublets. In this case, Higgs-strahlung type processes support the production of the lightest and the heaviest Higgs scalars only. With the diagonalizing matrix (29), one can compute the couplings of Higgs scalars to a $Z$ line. In fact, the second column of Table IV indicates these couplings. As we see, only the lightest Higgs $h_1$ can be produced in a Higgs-strahlung type process in NMSSM2. The heavier Higgs scalars cannot be obtained in such processes.

### D. Effects of the Radiative Corrections

The discussions above show that, in the limit of large Higgs trilinear couplings, both $Z'$ models and NMSSM approach a HTCDM in which all vacuum expectation values are of the same order. However, for a proper analysis of the particle spectrum it is necessary to investigate the effects of the radiative corrections on the stability of the HTCDM. Effects of the radiative corrections have already been discussed for $Z'$ models in [12], and NMSSM in [17]. The radiative effects of the entire particle spectrum on the Higgs potential could be parametrized by using the effective potential approximation. To one-loop accuracy the effective potential has the usual Coleman-Weinberg form

$$V_1 = V + \frac{1}{64\pi^2} Str\mathcal{M}^4 \ln\frac{\mathcal{M}^2}{Q^2} \tag{30}$$

where $\mathcal{M}$ is the Higgs field dependent mass-matrices of the fields entering the supertrace $Str = (-1)^{2J}(2J+1)Tr$. Here $Q$ is the renormalization scale. Generally, unless supersymmetry is broken below $\sim$ TeV the loop effects as well as the direct production of the supersymmetric particles are hard to detect in present and near future experiments. However, then the logarithms in the Coleman-Weinberg effective potential may not be satisfactorily large. In spite of this fact, this formula is still satisfactory for large enough Yukawa couplings (See the second reference in [9]). Among all supersymmetric particle spectrum especially top quark and top squarks are important due to the large value of top Yukawa coupling, $h_t \sim \sqrt{2}$. Then, taking only the dominant stop and top quark contributions into account, among all potential parameters only the following ones get significantly corrected:

$$\begin{aligned}
\hat{A}_s &= A_s + \beta_{h_t} S_{\tilde{t}Q} A_t \\
\hat{m}_2^2 &= m_2^2 + \beta_{h_t}\Big[(A_t^2 + A^2)S_{\tilde{t}Q} - A^2\Big]
\end{aligned}$$

$$\hat{\lambda}_{1s} = \lambda_{1s} + \beta_{h_t} S_{\tilde{t}Q} h_s^2 \qquad (31)$$
$$\hat{\lambda}_2 = \lambda_2 + \beta_{h_t} S_{\tilde{t}t} h_t^2$$

with

$$\beta_{h_t} = \frac{3}{(4\pi)^2} h_t^2$$
$$S_{\tilde{t}Q} = \ln \frac{m_{\tilde{t}_1} m_{\tilde{t}_2}}{Q^2} \qquad (32)$$
$$S_{\tilde{t}t} = \ln \frac{m_{\tilde{t}_1} m_{\tilde{t}_2}}{m_t^2}$$

where the last two quantities represent the splitting between stops and the scale $Q$, and top quark mass, respectively. $A_t$ is the top trilinear coupling coming from the superpotential (1) or (2), and the the remaining mass parameter $A^2$ is the sum of the soft mass-squareds of top squarks; $A^2 = m_{\tilde{Q}}^2 + m_{\tilde{U}}^2$. In deriving these one-loop corrections we assumed $m_{\tilde{Q}}^2 \sim m_{\tilde{U}}^2$ in accordance with the FCNC constraints [18], and expanded the stationarity conditions in powers of stop splitting $m_{\tilde{t}_2}^2 - m_{\tilde{t}_1}^2$. Detailed expressions for stop mass-squared matrix can be found in [12,17].

One recalls from the discussions of the tree-level potential that the existence of the Higgs trilinear coupling driven minimum of the potential can be characterized by the threshold value $A_s^{crit}$ of $A_s$. This threshold value of $A_s$ is highly precise if the sum of the soft mass-squareds of the Higgs fields are positive, and irrespective of the order of the transition potential possesses a HTCDM if $A_s$ is sufficiently large compared to $A_s^{crit}$. Thus, it is convenient to analyze the effects of the radiative corrections on the vacuum structure starting with a HTCDM at the tree-level. If $\mathcal{A}_s^{crit}$ is the critical value of $A_s$ in the presence of the radiative corrections, one has

$$\mathcal{A}_s^{crit} = \frac{A_s^{crit}}{1+\delta} \qquad (33)$$

where $\delta$ represents the effects of the radiative corrections, and can be expressed solely in terms of the Higgs- and top-trilinear couplings and the Yukawa couplings:

$$\begin{aligned}\delta = & \frac{1}{6}\beta_{h_t} S_{\tilde{t}Q}\Big[ -2 + 12\frac{A_t}{A_s} - 16\left(\frac{A_t}{A_s^{crit}}\right)^2 \Big] \\ & + \frac{1}{18}\beta_{h_t}(1 - S_{\tilde{t}Q})\Big[16\left(\frac{A_t^{crit}}{A_s^{crit}}\right)^2 + 3\left(\frac{A_t}{A_s^{crit}}\right)^2 \Big] \\ & - \frac{1}{3}\beta_{h_t} S_{\tilde{t}t}\left(\frac{h_t}{h_s}\right)^2 \end{aligned} \qquad (34)$$

where, following the discussion of CCB minima in MSSM in [19], we introduced the critical value of $A_t$ via the relation

$$A_t^{crit\,2} + 3\mu_s^2 = m_{\tilde{Q}}^2 + m_{\tilde{U}}^2 \qquad (35)$$

which represents the threshold value of $A_t$ for which color and/or charge breaking just starts taking place, for a given $\mu_s = \frac{h_s v_s}{\sqrt{2}}$. In these formuale, $A_s \geq A_s^{crit}$ and $A_t \leq A_t^{crit}$ if the vacuum state under concern is a non-CCB HTCDM. The exact value of $\delta$ requires a full specification of the scalar sector of the theory including the squark trilinear mass terms in superpotentials (1) or (2). The criterium induced by $\delta$ has a severe dependence on its sign: If $\delta < 0$, $\mathcal{A}_s^{crit} > A_s^{crit}$, and thus tree-level HTCDM might disappear if the actual value of $A_s$ were close to $A_s^{crit}$ at the tree level. In the opposite case of $\delta > 0$, $\mathcal{A}_s^{crit} < A_s^{crit}$ and HTCDM is supported by the radiative corrections. Since the Higgs VEV's are of the same order, satisfying the CDF value of the top-quark requires $h_t \sim \sqrt{2}$, so that effects of the radiative corrections are no way negligable. Moreover, for the reasonable set of parameters, $h_t \sim \sqrt{2}$, $A_t^{crit} \sim A_s^{crit}$, $Q^2 \sim m_t^2$, $m_{\tilde{t}_1} m_{\tilde{t}_2} \sim G_F^{-1}$ and $h_s \sim G$, $\delta$ turns out to be negative so that radiative corrections prefer $\mathcal{A}_s^{crit} > A_s^{crit}$ which can destabilize the vacuum state unless $A_s >> A_s^{crit}$ at the tree level. Radiative corrections modify mass matrices of all scalars, in particular that of the CP-even Higgs scalars by addition of the following matrix

$$(\delta\mathcal{M}^2)_h = \beta_{h_t} S_{\tilde{t}t} \begin{pmatrix} \mu_s A_t & -\mu_s A_t & \mu_s(2\mu_s - A_t) \\ -\mu_s A_t & 4m_t^2 & -\mu_s A_t \\ \mu_s(2\mu_s - A_t) & -\mu_s A_t & \mu_s A_t \end{pmatrix} \tag{36}$$

which is obtained by assuming $S_{\tilde{t}Q} \sim S_{\tilde{t}t}$, and a small stop splitting. In fact, one can write $S_{\tilde{t}t} = \ln(1 + (3/2)(h_s^2/h_t^2) + A_t^{crit\,2}/2m_t^2)$ using the definition of $A_t^{crit}$ (35). As $Q^2 \sim m_t^2$ is the natural renormalization scale, this approximation is reasonable. The entries of the tree-level mass matrices (14) of $Z'$ models, and (22) and (27) of NMSSM are now modified with the addition of (36). Let us note an important difference between $Z'$ models and NMSSM in terms of the behaviour of their mass matrices under radiative corrections. In $Z'$ models, (14), with its all elements are non-vanishing, gets non-vanishing contributions to each of its elements through the radiative corrections, preserving its form. On the other hand, in NMSSM, tree-level mass matrices, (22) and (27), already have some of their elements vanishing so that there is no mixing between the doublet and singlet contributions. However, with the addition of the radiative corrections (36), this simple tree-level picture is destroyed, and now singlet and doublet sectors do mix. Even in the limit of small $A_t$, $Re[H_1^0]Re[S^0]$ type mixing cannot be avoided.

If $A_s$ is sufficiently large compared to the radiatively corrected critical point $\mathcal{A}_s$ (33) then potential (3) will definitely have a HTCDM in which the VEV's are proportional to $A_s$ and their values are eventually fixed by the Fermi scale $G_F^{-1}$. Thus one can safely take VEV's equal in (36). Factoring out $G_F^{-1}/4$ from (36), one observes that $\mu_s^2$ and $m_t^2$ terms contribute by $0.08\, h_s^2 S_{\tilde{t}t}$ and $0.3 S_{\tilde{t}t}$, respectively. Thus, especially the top quark contribution is important. Although one can analytically obtain the effects of (36) on the mass spectrum and couplings, the results will be algebraically involved; and thus, we will numerically analyze the consequences of radiative corrections in the next section.

## III. HIGGS SEARCH VIA BJORKEN PROCESSES

The search for the Higgs particles is one of the most important issues at LEP2 and NLC. Though two-fermion processes are still of interest, the true novelty at high energy $e^+e^-$

colliders will come from four-fermion processes, among which the $s$-channel Higgs-strahlung process $e^+e^- \to ZH$ is the most important one for Higgs production. In fact, other processes in which Higgs is formed in $WW$ and $ZZ$ $t$- channel collisions have smaller cross sections at LEP2 energies, and their interference with the Higgs- strahlung type processes could be avoided by preventing $e$ and $\nu_e$ from the final products [7]. Above all, we should analyze four-fermion (4f) processes because intermediate state Higgs particles show up as resonances when their mass and the invariant mass flow to that channel coincide. In the much simpler process $e^+e^- \to ZH$ one cannot trigger the multi-Higgs structure of the models under concern as the products in a specific collision process are fixed. With these constraints in mind, we analyze the following four-fermion process

$$e^+e^- \to Z_i \to (Z_j \to \bar{f}_2 f_2) \;\; (h_k \to \bar{f}_1 f_1) \tag{37}$$

where, depending on the $e^+e^-$ CM energy $\sqrt{s}$, vector bosons and Higgs bosons above may come to the physical shell. Computation of the cross section for 4f processes like this is a highly complicated problem due to the phase space integration [20], and one mostly resorts to numerical techniques [7]. Despite this, however, we can extract the necessary information about the Higgs structure of the underlying models without performing a full calculation if we take the ratio of the differential cross section to that of the SM. Before going into the details of such a calculation it is convenient to describe the properties of $Z'$ models due to its complicated Higgs-vector boson sector. For $Z'$ models, in HTCDM, $Z - Z'$ mixing angle (9) is vanishingly small, and we assume it remains small also when radiative corrections are included. Assuming further $Z'$ be leptophobic, it is seen that $Z_2$ does not contribute to (37), so an analysis of (37) with $Z_1 \equiv Z$ is sufficient.

To calculate the total cross section $\sigma$ one needs to integrate over the phase space of the final particles, which is not possible by hand [7]. Moreover, in the case of polarized electron-positron beams task will be much more complicated. The amplitude for the scattering process (37) in the models under concern differs from that in the SM by the multitude of Higgs scalars reflecting them in $ZZh_k$ and $h_k\bar{f}_1 f_1$ couplings. This observation greatly simplifies the analysis if one integrates over first $\bar{f}_1$ and $f_1$ phase spaces using the momentum conservation, and identifies the remaining task to be done with that of the SM process. Then the ratio of the resulting cross section to that of the SM depends only on the invariant mass $p^2$ of the $\bar{f}_1 f_1$ system:

$$\frac{d\sigma_{Z',\,NMSSM}(p^2)}{d\sigma_{SM}(p^2)} \equiv I(p^2) = \mid \sum_k R_{ZZh_k}\mathcal{R}_{ak}\frac{p^2 - m_H^2 - im_H\Gamma_{SM}}{p^2 - m_{h_k}^2 - im_{h_k}\Gamma_k} \mid^2 \tag{38}$$

where $R_{ZZh_k}$ are $ZZh_k$ couplings, listed in Tables III and IV, in units of corresponding SM coupling $G/2$. Higgs-fermion couplings are parametrized by $a$, which can be 1 and 2 for down- and up-type fermions, respectively. Furthermore, $\Gamma_k$ and $\Gamma_{SM}$ designate the total widths of $h_k$ and $H$, respectively. $p^2$, invariant mass flowing into the Higgs branch, has the kinematical range of $4m_{f_1}^2$ to $(\sqrt{s} - 2m_{f_2})^2$. As $p^2$ varies in this range $I(p^2)$ will be sharply peaked at each $m_{h_k}$, as long as $m_{h_k}$ is kinematically accessible. Finally, one notices that $I(p^2)$ is independent of the beam polarizations.

For the compactness of the presentation, we introduce the dimensionless parameter $x^2 = p^2/M_H^2$ which equals unity when the SM Higgs mass resonance is encountered. In what

follows, we take $M_H$ equal to the lightest Higgs boson mass in the particular model under concern. In this sense, at $x = 1$ lightest Higgs resonance occurs. As $x$ gets higher and higher values other Higgs scalars with non-vanishing couplings will be excited in the order of increasing mass. For trilinear Higgs Yukawa coupling $h_s$, we assume $h_s \approx G$. Actually, $h_s$ can be choosen as low as $h_s^{min} \approx 0.36$ at which the present LEP lower bound of the lightest Higgs mass is exceeded at the tree level. For $h_s \sim G$, one gets $\mu_s \approx M_Z$, which is a reasonable scale. On the other hand, for $g_{Y'}$ we assume the usual GUT constraint of $g_{Y'} \sim \sqrt{5/3} g_Y$. The $S^3$ Yukawa coupling $k_s$ is either $\sim h_s$ (NMSSM1), or $<< h_s$ (NMSSM2). For $|k_s A_k| << |h_s A_s|$, as is necessary for obtaining HTCDM, $A_k$ dependence of the masses and the couplings cancel, as was illustrated before. In addition to these, we take $|A_t| << \mu_s$, so that $A_t$ dependence of the radiative corrections to the CP-even Higgs mass-squared matrix (36) can be neglected. Finally, we approximate $\Gamma_{SM}$ by $\Gamma(H \to \bar{b}b) + \Gamma(H \to \bar{c}c)$, and assume all scalars have the same width. This last assumption is falsified especially when the Higgs mass exceeds $M_Z$, but it does not affect the main conclusion of the work because the width of a particular resonance is not of central concern. At the final state we take $f_1 = b$ and $f_2 = \mu$, which is convenient for detection purposes at LEP2 [7].

With the above mentioned values of parameters, one can calculate all couplings and masses. In fact, tree- and loop- level values of the lightest Higgs mass are tabulated in Table V, for $Z'$ models, and NMSSM for both cases in (19). An analysis of $I(x)$ (38) reveals that it is necessary to have $\sqrt{s} \geq 350$ GeV for all Higgs scalars be excited in both models. This value of $\sqrt{s}$ is pretty much above the maximum value of 205 GeV aimed at LEP2, and thus one is to wait for NLC operation for the experimental realization of these scalar spectra, if any.

In Fig. 1 we show $I(x)$ for $Z'$ models, at $\sqrt{s} = 350$ GeV, with and without the radiative corrections. Here dashed curve represents the tree-level analysis, and as expected there is a single resonance curve at $x \approx 2.1$ corresponding to the heaviest Higgs whose coupling is given in Table II. In this graph, the full curve shows $I(x)$ when radiative corrections are included. Under radiative corrections none of the couplings remains vanishing, and therefore, effects of the scalars which were inert at the tree level show up. In this sense, the first resonance curve at $x \approx 1.2$ corresponds to the next-to-lightest Higgs which was absent in the tree- level $I(x)$. That this resonance is much narrower than that of the heaviest Higgs located at $x \approx 2$ is caused by the smallness of $R_{Z\,Z\,h_2}$. Both tree- and loop-level $I(x)$ has a non-negligable value at $x = 1$ because of the fact that lightest Higgs is observable at the tree-level and has still a large enough coupling at the loop level.

In Fig. 2 we present $I(x)$ for NMSSM1 described in equation (19). At the tree-level, in accordance with Table IV, only next-to-lightest Higgs is observable as is evidenced by the resonance at $x \approx 1.6$. Both dashed and full curves have vanishingly small values at $x \approx 1$ due to the fact that $R_{Z\,Z\,h_1}$, which vanishes at the tree-level, is still small compared to $R_{Z\,Z\,h_2}$. When radiative corrections are included place of the next-to-lightest Higgs resonance practically remains the same, and there is a tiny resonance curve at $x \sim 1.83$ representing the heaviest Higgs contribution. Such a narrow resonance is caused by the smallness of $R_{Z\,Z\,h_3}$ compared to $R_{Z\,Z\,h_2}$.

In Fig. 3 $I(x)$ for NMSSM2 is depicted. At the tree-level, in accordance with Table IV, only the lightest Higgs observable so that the dashed line $I(x) \approx 0.5$ arises. Differently than

the models analyzed in Figs. 1 and 2 in this model radiative corrections cause important modifications in the spectrum. This is mainly caused by the smallness of the elements of the mass-squared matrix compared to the two cases discussed above which make them more sensitive to the radiative corrections. Consequently, when the radiative corrections are included next-to-lightest Higgs is seen to have dominant couplings compared to others, so that aymptotics of the full curve are entirely determined by $h_2$. In fact, $I(x)$ has vanishingly small values at $x \approx 1$ and $x \approx 1.4$ due to this reason. The resonance curves of $h_2$ and $h_3$ are close to each other, narrower than tree-level ones of the previous cases, and located at $x \approx 1.1$ and $x \approx 1.3$, respectively.

## IV. CONCLUSIONS AND DISCUSSIONS

The analysis carried out in this work primarily concentrates on the similarities and dissimilarities between the $Z'$ models and NMSSM concerning their neutral Higgs scalars. The two models have been comparatively analyzed in that minimum of the potential characterized by the large values of trilinear soft mass coupling the SM singlet and the Higgs doublets. The issue of radiative corrections deals essentially with the stability of this minimum together with the corresponding Higgs mass–squared matrix. The radiative corrections are conveniently parametrized using the effective potential approximation. As a case study we analyzed Higgs production via Bjorken process at an $e^+e^-$ collider. Both models are comparatively analyzed referring basically to the variation of the cross section with the di-fermion invariant mass.

Once a high energy collider is given there appear several scattering processes whose signature necessarily depend on the details of the underlying model. This becomes especially clear after a comparative study of the SM and MSSM, for example, at $e^+e^-$ linear colliders [22]. On the other hand, characteristic to all supersymmetric models, there are sfermions, charginos, neutralinos, and fermions in addition to the Higgs particles whose distinguishability needs be studied. The two minimal extensions of the MSSM, that is, $Z'$ models and NMSSM, are already already distinguishable from the MSSM and 2HDM in terms of their particle spectrum. Moreover, there are also differences between $Z'$ models and NMSSM as they have different number of neutral gauge bosons (two for the former, one for the latter), psedoscalars (one for the former, two for the latter), and neutral gauginos (three for the former, two for the latter). Therefore, for processes with such signature, it can be easy to know what model is the underlying one. For example, the neutralino pair production, $e^+e^- \to \chi_i^0\chi_j^0$ or associated Higgs production $e^+e^- \to H_iP_i$ ($P$ is a pseudoscalar) are candidate processes. Despite such differences, however, the two models have equal number of CP–even Higgs particles. The primary goal of the future colliders is the discovery of the Higgs particle whose most likely production mode is the Bjorken process. That this process does not involve the pair production of the supersymmetric particles is especially appealing as it could be realized for moderate collider energies. Due to the reasons mentioned above, a discussion of the distinguishability of the CP–even Higgs scalars of the $Z'$ models and NMSSM is an important issue by itself. We have concentrated here on HTCDM (where $Z'$ models are likely to have for satisfying the LEP constraints) in which the Higgs potentials of the two model are similar apart from their respective parameters. The re-

sults of the analysis are presented in the tabels and figures for both tree–level and one–loop Higgs potentials. NMSSM, having no gauge extension at all, is particularly interesting in HTCDM. For example, a glance at Table IV shows that these couplings are identical to those of the minimal model. However, one–loop $R_{ZZh_i}$ couplings for both NMSSM1 and NMSSM2 destroy this tree–level picture by causing other couplig to have non–vanishing values. Then, as suggested by Figs. 2 and 3 there appear new resonances allowing, eventually, for distinguishability. This examplifying case particularly shows how important the radiative corrections are. At the tree level, there is a certain hierarchy, in particular, some couplings vanish identically as shown in Tables 3 and 4. However, the radiative corrections are strong enough to elevate other couplings to non-vanishing values. This is particularly observed in the figures (solid curves) where there arise additional resonances compared to the tree–level results (dashed curve) corresponding to additional excited Higgs bosons due to their raditively induced couplings.

In Sec. III we have considered only $2 \to 4$ fermion processes in illustrating Higgs search via the Bjorken mechanism. The actual experimental search strategy [7] is to look for $f_2 = \nu$ and $f_1 = b$ in eq. (37), which kills down the possibility of having a pseudoscalar boson coupling to $\bar{f}_2 f_2$ pair. Such an event selection mechanism necessarly establishes the existence of a scalar or set of scalars as the collider energy increases. However, when the collider energy gets higher and higher, pairs of lightest neutralinos and charginos will be produced in association with the Higgs. In this case $Z$ and $P$ couplings to $\bar{f}_2 f_2$ pair compete for $h_s \sim G$ as has been assumed throughout the work. In spite of all such supersymmetric particle production modes occuring in association with a CP–even Higgs particle, the main search mecanishm for the CP–even Higgs remains to be the Bjorken process with $f_2 = \nu$ and $f_1 = b$ [7].

As a final point, it is obvious that $I(p^2)$ described in the figures is not a directly measurable quantity. However, it is highly useful in distinguishing the two models in terms of the di-fermion invariant mass. Indeed, $I(p^2)$ could be a useful tool in MONTE CARLO simulations of these models in the next linear collider [21]. Both the simulation studies (with more sophistcated numerical techniques) and analysis of the experimental data can be guided by the results of this analysis.

## V. ACKNOWLEDGEMENTS

The author is grateful to Goran Senjanovic for highly stimulating discussions and helpful comments. He also acknowledges the discussions with Alejandra Melfo.

# REFERENCES


[1] F. Franke, H. Fraas, Int.J.Mod.Phys. **A12** (1997) 479; U. Ellwanger, M. Rausch de Traubenberg, C. A. Savoy, Nucl. Phys. **B492** (1997) 21; F. Franke, H. Fraas, Phys. Lett. **B353** (1995) 234; U. Ellwanger, M. Rausch de Traubenberg, C. A. Savoy Z. Phys. **C67** (1995) 665; J. Ellis, J. F. Gunion, H. E. Haber, L. Roszkowski, F. Zwirner, Phys. Rev. **D39** (1989) 844; M. Drees, Int. J. Mod. Phys. **A4** (1989) 3635.

[2] M. Cvetic, D. A. Demir, J. R. Espinosa, L. Everett, P. Langacker, Phys. Rev. **D56** (1997) 2861

[3] M. Cvetic and P. Langacker, Phys. Rev. **D54** (1996) 3570; Mod. Phys. Lett. **A11** (1996) 1247; G. Cleaver, M. Cvetic, J. R. Espinosa, L. Everett, P. Langacker, Phys. Rev. **D57** (1998) 2701.

[4] J. R. Espinosa, Nucl. Phys. Proc. Suppl. **62** (1998) 187; J. L. Hewett, T. G. Rizzo, Phys. Rep. **183** (1989) 193; J. Ellis, K. Enqvist, D. V. Nanopoulos, F. Zwirner, Nucl. Phys. **B276** (1986) 14.

[5] G. D'Agostini, G. Degrassi, hep-ph/9902226; M. S. Chanowitz, Phys. Rev. **D59** (1999) 073005; J. Ellis, G. L. Fogli, E. Lisi, Phys. Lett. **B389** (1996) 321.

[6] J. A. Bagger, A. F. Falk, M. Swartz, hep-ph/9908327; K. Hagiwara, S. Matsumoto, D. Haidt, C. S. Kim, Z. Phys. **C64** (1994) 559; M. Veltman, Nucl. Phys. **B123** (1977) 89.

[7] ALEPH, DELPHI, L3 and OPAL Collaborations, OPAL Technical Note TN-614 (July 13 1999) submitted to Tampere 99, July 15-21, Tampere, Finland.

[8] B. A. Kniehl, Phys. Rep. **240** (1994) 211; A. Denner, J. Kublbeck, R. Mertig, M. Bohm Z. Phys. **C56** (1992) 261; Fleischer, F. Jegerlehner, Nucl. Phys. **B216** (1983) 469; J. Ellis, M. K. Gaillard, D. V. Nanopoulos, Nucl. Phys. **B106** (1976) 292 ; B. L. Ioffe, V. A. Khoze, Sov. J. Part. Nucl. **9** (1978)50 ; B. W. Lee, C. Quigg, H. B. Thacker, Phys. Rev. **D16** (1977) 1519.

[9] J. Rosiek, A. Spoczak, Phys. Lett. **B341** (1995) 419; P.H. Chankowski, S. Pokorski, J. Roziek, Phys. Lett. **B286** (1992) 307, **B281** (1992) 100; A. Brignole, J. Ellis, G. Ridolfi, F. Zwirner, Phys. Lett. **B271** (1991) 123; J. Ellis, G. Ridolfi, F. Zwirner, Phys. Lett. **B262** (1991) 477; R. Barbieri, M. Frigeni, Phys. Lett. **B258** (1991) 395;J. Ellis, G. Ridolfi, F. Zwirner, Phys. Lett. **B257** (1991) 83.

[10] Ya. B. Zeldovich, I. Yu. Kobzarev, L. B. Okun, Sov. Phys. JETP **40** (1975) 1; A. Vilenkin, Phys. Rep. **121** (1985) 263.

[11] J. Bagger, E. Poppitz, Phys. Rev. Lett. **71** (1993) 2380; B. Rai, G. Senjanovic, Phys. Rev. **D49** (1994) 2729.

[12] D. A. Demir, N. K. Pak, Phys. Rev. **D57** (1998) 6609.

[13] F. Abe et. al., CDF Collab., Phys. Rev. Lett. **79** (1997) 2191.

[14] D. A. Demir, Phys. Rev. **D59** (1999) 015002.

[15] X. Li, E. Ma, J.Phys. **G23** (1997) 885; E. Ma, D. Ng, Phys. Rev. **D49** (1994) 6164; T. V. Duong, E. Ma, Phys. Lett. **B316** (1993) 307; E. Keith, E. Ma, Phys. Rev. **D54** (1996) 3587; E. Keith, E. Ma, Phys. Rev. **D56** (1997) 7155.

[16] A. E. Faraggi, Phys. Lett. **B274** (1992) 47, *ibid.*, **B377** (1996) 43.

[17] U. Ellwanger, M. Rausch de Traubenberg, C. A. Savoy, Phys. Lett. **B315** (1993) 331; T. Elliot, S. F. King, P. L. White, Phys. Lett. **B351** (1995) 213; S. F. King, P. L. White Phys. Rev. **D52** (1995) 4183.

[18] J. S. Hagelin, S. Kelly, T. Tanaka, Nucl. Phys. **B415** (1994) 293.
[19] J. A. Casas, A. Lleyda, C. Munoz, Nucl. Phys. **B471** (1996) 3.
[20] D. A. Demir, N. K. Pak, Phys. Lett. **B439** (1998) 309; **B411** (1997) 292.
[21] NLC ZDR Design Group, NLC Physics Working Groups, hep-ex/9605011.
[22] ECFA/DESY LC Physics Working Group, Phys. Rep. **299** (1998) 1.

| Quantity | $Z'$ Models | NMSSM |
|---|---|---|
| $\lambda_1$ | $G^2/8 + {g_{Y'}}^2 Q_1^2/2$ | $G^2/8$ |
| $\lambda_2$ | $G^2/8 + {g_{Y'}}^2 Q_2^2/2$ | $G^2/8$ |
| $\lambda_S$ | ${g_{Y'}}^2 Q_S^2/2$ | $k_s^2$ |
| $\lambda_{12}$ | $-G^2/4 + {g_{Y'}}^2 Q_1 Q_2 + h_s^2$ | $-G^2/4 + h_s^2$ |
| $\lambda_{1S}$ | ${g_{Y'}}^2 Q_1 Q_S + {h_s}^2$ | $h_s^2$ |
| $\lambda_{2S}$ | ${g_{Y'}}^2 Q_2 Q_S + {h_s}^2$ | $h_s^2$ |
| $\lambda_{S12}$ | 0 | $h_s k_s$ |
| $\tilde{\lambda}_{12}$ | $-h_s^2 + g_2^2/2$ | $-h_s^2 + g_2^2/2$ |

TABLE I. Explicit expressions for quartic couplings in $Z'$ models and NMSSM.

| $Z_i$ | $g_V^{(i)}$ | $g_A^{(i)}$ |
|---|---|---|
| $Z_1$ | $(\epsilon_L^f + \epsilon_R^f)\cos\theta - \kappa(\epsilon'^f_L + \epsilon'^f_R)\sin\theta$ | $(\epsilon_L^f - \epsilon_R^f)\cos\theta - \kappa(\epsilon'^f_L - \epsilon'^f_R)\sin\theta$ |
| $Z_2$ | $(\epsilon_L^f + \epsilon_R^f)\sin\theta + \kappa(\epsilon'^f_L + \epsilon'^f_R)\cos\theta$ | $(\epsilon_L^f - \epsilon_R^f)\sin\theta + \kappa(\epsilon'^f_L - \epsilon'^f_R)\cos\theta$ |

TABLE II. $Z_i f \bar{f}$ couplings in $Z'$ models. Here $\kappa = g_{Y'}/G$. To obtain these couplings in NMSSM, one sets $g_{V,A}^{(2)} = 0$, $\kappa = 0$, and $\theta = 0$.

| $h_k$ | $Z_1\, Z_1$ | $Z_2\, Z_2$ | $Z_1\, Z_2$ |
|---|---|---|---|
| $h_1$ | $\frac{1}{\sqrt{6}} G\, M_Z$ | $\frac{1}{\sqrt{6}} 3\, G\, M_Z \rho^2$ | 0 |
| $h_2$ | 0 | 0 | $-\frac{1}{2} G\, M_Z \rho$ |
| $h_3$ | $-\frac{1}{\sqrt{12}} G\, M_Z$ | $\frac{1}{\sqrt{12}} 3\, G\, M_Z \rho^2$ | 0 |

TABLE III. $Z_i Z_j h_k$ couplings in $Z'$ models. Here $\rho = 2(g_{Y'}/G)Q_1$.

| $h_k$ | $Z\,Z$ (NMSSM1) | $Z\,Z$ (NMSSM2) |
|---|---|---|
| $h_1$ | 0 | $\frac{1}{2}G\,M_Z$ |
| $h_2$ | $\frac{1}{2}G\,M_Z$ | 0 |
| $h_3$ | 0 | 0 |

TABLE IV. $Z\,Z\,h_k$ couplings in NMSSM1 and NMSSM2 (see Eq. (19)).

| $m_{h_1}$ (GeV) | $Z'$ Models | NMSSM1 | NMSSM2 |
|---|---|---|---|
| Tree Level | 121.8 | 126.0 | 121.8 |
| One-Loop | 127.5 | 132.9 | 121.3 |

TABLE V. Lightest Higgs mass in the models under concern.

## Figure Captions

Fig. 1. Normalized cross section differential $I(x)$ for $Z'$ models at tree- (dotted curve) and one-loop (full curve) levels.
Fig. 2. Same as in Fig. 1, but for NMSSM1.
Fig. 3. Same as in Fig. 1, but for NMSSM2.

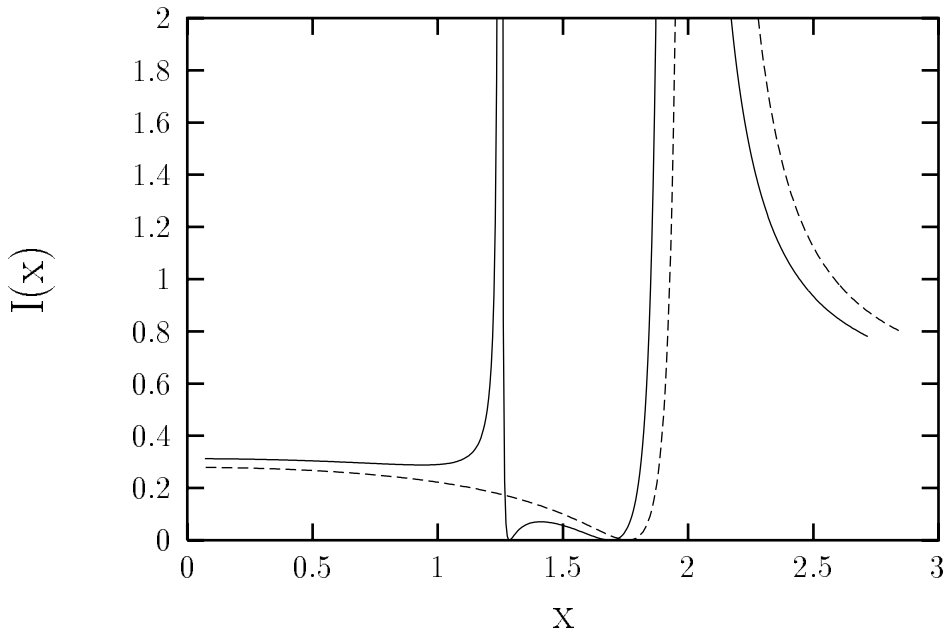


Figure 1

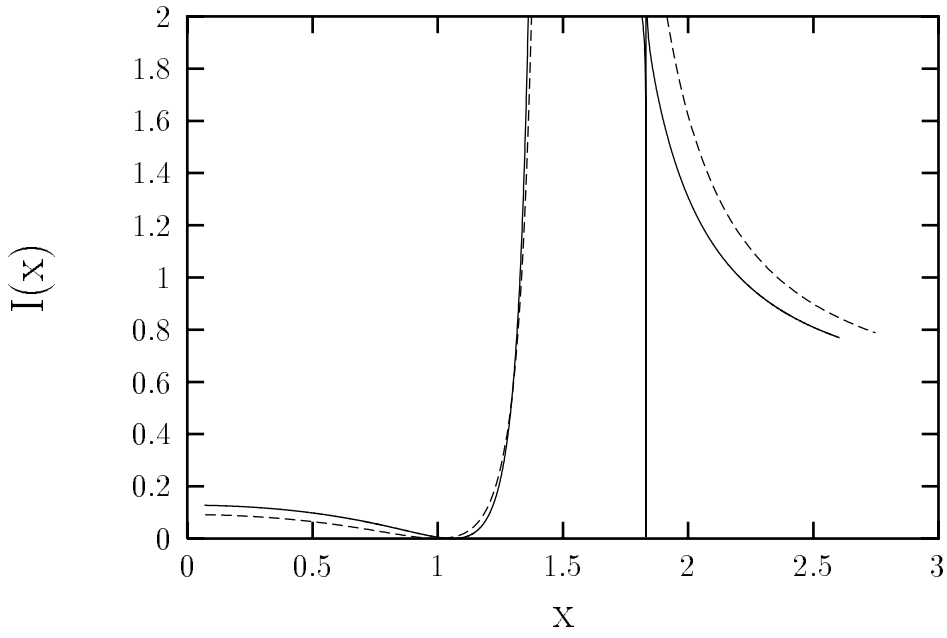


Figure 2

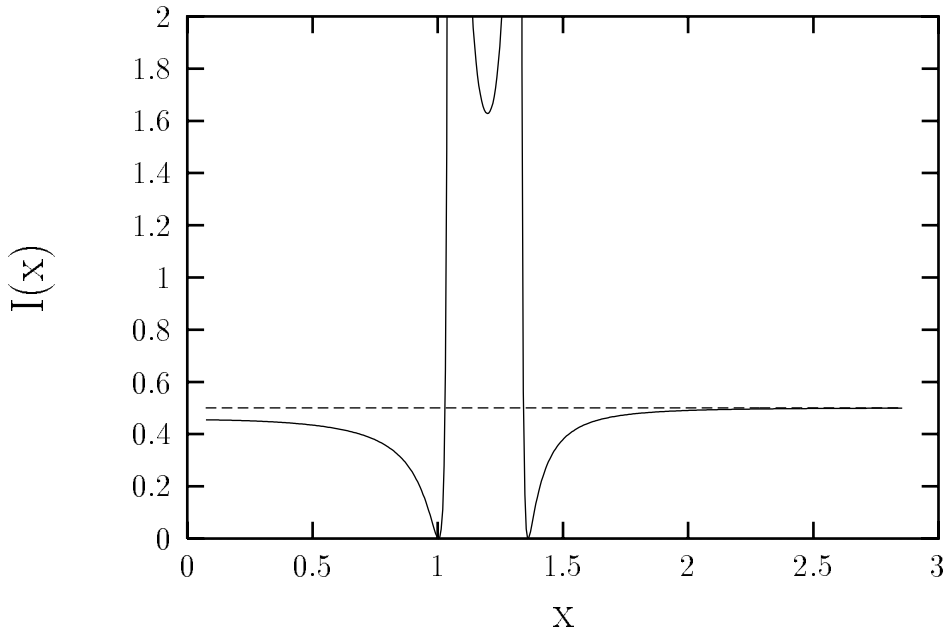


Figure 3